Optimization of SNR Improvement in the Noncoherent OTDR Based on Simplex Codes

Duckey Lee, Hosung Yoon, *Member, IEEE*, Pilhan Kim, Jonghan Park, and Namkyoo Park, *Member, IEEE*

***Abstract*—This paper demonstrates signal-to-noise ratio (SNR) improvement of an optical time-domain reflectometer (OTDR) using simplex codes (scs) for the first time. By developing a generalized procedure for the analysis of noise transfer in the coded OTDR employing L-bit scs, the SNR dependence on the receiver bandwidth is also investigated. Experimental results obtained from a constructed sc-OTDR showed excellent agreement with theoretical results over entire code lengths. Improvement of the SNR up to 9.2 dB has been demonstrated using 255-bit scs.**

***Index Terms*—Coding gain, optical fiber communications, optical time-domain reflectometer (OTDR), simplex codes (scs).**

I. Introduction

An OPTICAL time-domain reflectometer (OTDR) characterizes optical fibers by injecting an optical probe pulse into the fiber under test and detecting the backscattered optical signals. Increasing the pulsewidth of the probe pulse improves the signal-to-noise ratio (SNR) of the detected signal and accordingly improves the dynamic range but degrades the spatial resolution of the OTDR. To overcome this tradeoff between the SNR and the spatial resolution, the use of correlation techniques—commonly used in wireless radars—have been suggested, e.g., employing periodic pseudorandom bit sequences (PRBSs) [1], [2]. Still, with the problem resulting from the periodic features of PRBS, this approach was found to be unsuitable for the practical applications [3].

Overcoming the limitations of PRBS-coded OTDR, the complementary correlation OTDR (cc-OTDR) based on the Golay codes was suggested [4]. Following the cc-OTDR, an OTDR based on the simplex codes (scs) was then proposed [5], predicting better SNR performances (over the Golay-code cc-OTDR) without the penalty in the spatial resolution. Still, with the analysis based on simple analogy—compared to that of optical spectrometry [6], [7]—the scope of the work was limited to a conjecture on the expected amount of coding gain (SNR increase over conventional OTDR, with identical measurement time and spatial resolution). Considering the need of detailed guidelines for its practical application, a systematic analysis—with considerations on OTDR-specific hardware and supporting experimental data—should be provided to give insights for the initial design consideration.

In this work, we develop a generalized procedure for the performance analysis of sc-OTDR, to fully analyze its noise characteristics and to provide practical guidelines for the construction of such an OTDR. We also experimentally demonstrate the SNR improvement in sc-OTDR by constructing an OTDR board with pulse modulation/decoding capability. Experiments have been performed using $7 \sim 255$-bit scs supporting the theory, with excellent agreement over the entire code lengths.

II. Time-Domain Application of Hadamard Transform

The S matrix has been used for noise reduction in optical spectrometry [6], [7]. Briefly, the S matrix is a unipolar matrix composed of 1's and 0's, and the rows of this matrix are called scs. This matrix can be also derived from a normalized Hadamard matrix, a bipolar matrix composed of 1's and -1's [7]. The S matrix, due to its unipolar characteristics, has been generally applied in the detection of optical power signals, although it provides a lower efficiency than the Hadamard matrix. The operation using Hadamard or S matrix is called the Hadamard transform, which has been carried out by a fast algorithm—fast Hadamard transform (FHT) [8]. Traditionally, the Hadamard-transform technique has been applied to the spectrometry by using a spatial mask having holes and blocks [7].

Instead of using the spatial mask, the technique also can be applied to an OTDR system by turning the laser ON and OFF in the time domain, to represent 1's and 0's in the S matrix. As an example, we illustrate in Fig. 1 the time-domain equivalent of the S matrix (order 3). Defining $\psi_1(t)$ as an OTDR trace, measured with a single probe pulse $P_1(t)$, we also set $\psi_2(t)$ and $\psi_3(t)$ to be the traces measured with the time-delayed probe pulses $P_2(t) = P_1(t-\tau)$ and $P_3(t) = P_1(t-2\tau)$, respectively [τ : pulsewidth of $P_1(t)$]. Fig. 1(a) shows that the following relationships should be satisfied between these time-delayed pulses traces.

$$P_2(t) = P_1(t-\tau), \quad P_3(t) = P_1(t-2\tau)$$
$$\psi_2 = \psi(t-\tau), \quad \psi_3(t) = \psi_1(t-2\tau). \tag{1}$$

Manuscript received December 22, 2004; revised July 1, 2005.

D. Lee was with the Optical Communications Systems Laboratory, School of Electrical Engineering and Computer Science, Seoul National University, Seoul, Korea 151-742. He is now with Korea Telecom, Seoul, Korea (e-mail: duckey@ieee.org).

H. Yoon, P. Kim, J. Park, and N. Park are with the Optical Communication Systems Laboratory, School of Electrical Engineering and Computer Science, Seoul National University, Seoul, Korea, 151-742 (e-mail: danny@stargate.snu.ac.kr; phkim@stargate.snu.ac.kr; jonghan@stargate.snu.ac.kr; nkpark@plaza.snu.ac.kr).

Digital Object Identifier 10.1109/JLT.2005.859437

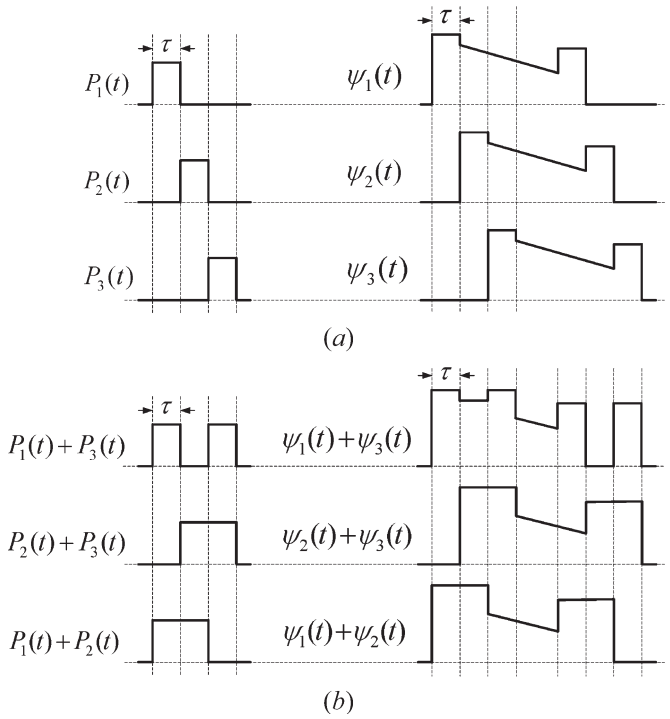

Fig. 1. Application of Hadamard transform to the OTDR in the time domain.

Under these arrangements, three coded traces $\eta_1(t)$, $\eta_2(t)$, and $\eta_3(t)$ can be measured by launching coded pulse sequences into the fiber [Fig. 1(b)] as follows:

$$\begin{aligned} P_1(t)+P_3(t) &\Rightarrow \eta_1(t)=\psi_1(t)+\psi_3(t)+e_1(t) \\ P_2(t)+P_3(t) &\Rightarrow \eta_2(t)=\psi_2(t)+\psi_3(t)+e_2(t) \\ P_1(t)+P_2(t) &\Rightarrow \eta_3(t)=\psi_1(t)+\psi_2(t)+e_3(t) \end{aligned} \tag{2}$$

or equivalently

$$\begin{pmatrix}\eta_1(t)\\ \eta_2(t)\\ \eta_3(t)\end{pmatrix} = \mathbf{S}\begin{pmatrix}\psi_1(t)\\ \psi_2(t)\\ \psi_3(t)\end{pmatrix} + \begin{pmatrix}e_1(t)\\ e_2(t)\\ e_3(t)\end{pmatrix}$$

$$\mathbf{S} = \begin{pmatrix}1 & 0 & 1\\ 0 & 1 & 1\\ 1 & 1 & 0\end{pmatrix} \tag{3}$$

where $e_1(t)$, $e_2(t)$, and $e_3(t)$ correspond to the amplitudes of the receiver noise in each measurement, and $\mathbf{S}$ is the S matrix of order 3.

To recover the conventional OTDR trace $\psi_1(t)$, we apply the inverse Hadamard transform to the measured three (coded) traces, utilizing the following equations [here, $\hat{\psi}_i(t)$ represents the estimate of $\psi_i(t)$]:

$$\begin{aligned}\begin{pmatrix}\hat{\psi}_1(t)\\ \hat{\psi}_2(t)\\ \hat{\psi}_3(t)\end{pmatrix} &= \mathbf{S}^1\begin{pmatrix}\eta_1(t)\\ \eta_2(t)\\ \eta_3(t)\end{pmatrix} \\ &= \frac{1}{2}\begin{pmatrix}1 & -1 & 1\\ -1 & 1 & 1\\ 1 & 1 & -1\end{pmatrix}\begin{pmatrix}\eta_1(t)\\ \eta_2(t)\\ \eta_3(t)\end{pmatrix}.\end{aligned} \tag{4}$$

Explicitly including the noise terms, the expression is as follows:

$$\begin{aligned}\hat{\psi}_1(t) &= \frac{1}{2}\{\eta_1(t)-\eta_2(t)+\eta_3(t)\} \\ &= \psi_1(t)+\frac{e_1(t)-e_2(t)+e_3(t)}{2} \\ \hat{\psi}_2(t) &= \frac{1}{2}\{-\eta_1(t)+\eta_2(t)+\eta_3(t)\} \\ &= \psi_2(t)+\frac{-e_1(t)+e_2(t)+e_3(t)}{2} \\ \hat{\psi}_3(t) &= \frac{1}{2}\{\eta_1(t)+\eta_2(t)-\eta_3(t)\} \\ &= \psi_3(t)+\frac{e_1(t)+e_2(t)-e_3(t)}{2}.\end{aligned} \tag{5}$$

Now, averaging these estimates after inversely time shifting with multiples of τ and utilizing the time relationships in (1), we finally obtain the restored trace in (6), shown at the bottom of the next page.

Calculating the mean square error (mse) of the restored trace, we then get

$$\begin{aligned} &E\left\{\left(\frac{\hat{\psi}_1(t)+\psi_2(t+\tau)+\psi_3(t+2\tau)}{3}-\psi_1(t)\right)^2\right\} \\ &\quad=\frac{9\sigma^2}{36}=\frac{1}{4}\sigma^2 \\ &\quad\because E\{e_i(t+\varsigma)\}=0,\ E\left\{e_1^2(t+\varsigma)\right\}=\sigma^2(i=1,2,3) \\ &\quad E\{e_i(t)e_j(t+\varsigma)\}=0\,((i\neq j)\text{ or }(i=j,\ \varsigma\neq 0)) \end{aligned} \tag{7}$$

where E is the time average function. For the derivation of (7), we assumed that the receiver noise $e_i(t)$'s are uncorrelated zero-mean random processes with variance σ^2. Note that since the restored trace in (6) was obtained from the measurement of three coded traces, we have to compare its noise power to that of the conventional OTDR with $N=3$ (simple averaging of three identical single-pulsed measurements). As the mse of $N=3$ averaging process is simply $\sigma^2/3$, we get the following SNR improvement (coding gain over the conventional single-pulse averaging OTDR, with identical measurement time and spatial resolution) for the sc-OTDR, at the code length $L=3$.

$$\frac{\sqrt{\frac{\sigma^2}{3}}}{\sqrt{\frac{\sigma^2}{4}}}=\frac{2}{\sqrt{3}}. \tag{8}$$

III. Generalization to Arbitrary Code Length

The above example can be extended to the generalized case of code length L, as detailed below. Writing $\mathbf{S}_L$ and $\mathbf{S}_L^{-1}$ as the

S matrix and its inverse matrix of order L, trace estimates can be written as

$$\begin{pmatrix} \hat{\psi}_1(t) \\ \hat{\psi}_2(t) \\ \vdots \\ \hat{\psi}_L(t) \end{pmatrix} = \mathbf{S}_L^{-1} \begin{pmatrix} \eta_1(t) \\ \eta_2(t) \\ \vdots \\ \eta_L(t) \end{pmatrix} = \begin{pmatrix} \psi_1(t) \\ \psi_2(t) \\ \vdots \\ \psi_L(t) \end{pmatrix} + \mathbf{S}_L^{-1} \begin{pmatrix} e_1(t) \\ e_2(t) \\ \vdots \\ e_L(t) \end{pmatrix}. \tag{9}$$

Now, inversely time shifting each row in (9) with multiples of τ, and then introducing matrix $\mathbf{T}_L$ (normalized matrix of $\mathbf{S}_L^{-1}$), we obtain the following equations:

$$\begin{pmatrix} \hat{\psi}_1(t) \\ \hat{\psi}_2(t+\tau) \\ \vdots \\ \hat{\psi}_L\left(t+(L-1)\tau\right) \end{pmatrix} = \begin{pmatrix} \psi_1(t) \\ \psi_2(t+\tau) \\ \vdots \\ \psi_L\left(t+(L-1)\tau\right) \end{pmatrix} + \frac{2}{L+1}\mathbf{T}_L \begin{pmatrix} e_1(t) \\ e_2(t+\tau) \\ \vdots \\ e_L\left(t+(L-1)\tau\right) \end{pmatrix}$$

where

$$\mathbf{T}_L = \frac{L+1}{2}\mathbf{S}_L^{-1}, \quad T_{j,k} \in \{1,-1\}. \tag{10}$$

Now, utilizing the following relation extended from (1)

$$\psi_i\left(t+(i-1)\tau\right) = \psi_1(t) \qquad (i=1,2,\ldots,L) \tag{11}$$

we obtain L equations relating the estimate $\psi_i(t)$ to the conventional trace $\psi_1(t)$.

$$\begin{aligned} \hat{\psi}_1(t) &= \psi_1(t) + \frac{2}{L+1}\sum_{k=1}^{L} T_{1,k}e_k(t) \\ \hat{\psi}_2(t+\tau) &= \psi_1(t) + \frac{2}{L+1}\sum_{k=1}^{L} T_{2,k}e_k(t+\tau) \\ &\vdots \\ \hat{\psi}_L\left(t+(L-1)\tau\right) &= \psi_1(t) + \frac{2}{L+1}\sum_{k=1}^{L} T_{L,k}e_k \\ &\quad \times \left(t+(L-1)\tau\right). \end{aligned} \tag{12}$$

Finally, summing over the traces and taking its average, we obtain the following equation for the final trace, which includes the exact noise components:

$$\frac{1}{L}\sum_{k=1}^{L}\hat{\psi}_k\left(t+(k-1)\tau\right) = \psi_1(t) + \frac{2}{L(L+1)}\sum_{j=1}^{L}\sum_{k=1}^{L} T_{j,k}e_k\left(t+(L-1)\tau\right). \tag{13}$$

Now, calculating the mse of the restored trace

$$\begin{aligned} &E\left\{\left(\frac{1}{L}\sum_{k=1}^{L}\hat{\psi}_k\left(t+(k-1)\tau\right)-\psi_1(t)\right)^2\right\} \\ &= \frac{4}{L^2(L+1)^2}E\left\{\left(\sum_{j=1}^{L}\sum_{k=1}^{L}T_{j,k}e_k\left(t+(L-1)\tau\right)\right)^2\right\} \\ &= \frac{4}{L^2(L+1)^2}\left\{L^2\sigma^2 - \sum_{i=1}^{L-1}(L-i)R_N(i\tau)\right\} \\ &= \frac{4}{(L+1)^2}\left\{\sigma^2 - \frac{1}{L^2}\sum_{i=1}^{L-1}(L-i)R_N(i\tau)\right\}. \end{aligned} \tag{14}$$

Note that the above result was derived by using the following assumptions:

$$\begin{aligned} E\left\{e_i(t+\zeta)\right\} &= 0 \\ E\left\{e_i^2(t+\zeta)\right\} &= \sigma^2 \\ E\left\{e_i(t)e_j(t+\zeta)\right\} &= 0 (i \neq j) \\ E\left\{e_i(t)e_i(t+\zeta)\right\} &= R_i(\zeta) \\ &= R_N(\zeta), \qquad (i=1,2\ldots,L) \end{aligned} \tag{15}$$

i.e., the noise in the receiver is an independent identically distributed (i.i.d.) and wide sense stationary (w.s.s.) random process with zero mean—together with the interesting property of the matrix $\mathbf{T}_L$—in (16): The sum of elements in each row is always -1.

$$\sum_{k=1}^{L} T_{j,k} = -1 \qquad (j=1,2,\ldots,L) \tag{16}$$

Restricting our analysis to an ideal receiver with an infinite bandwidth, the mse in (14) can be simplified [for this case, note

---

$$\frac{\hat{\psi}_1(t)+\psi_2(t+\tau)+\psi_3(t+2\tau)}{3} = \psi_1(t) + \frac{e_1(t)-e_2(t)+e_3(t)}{6} + \frac{-e_1(t+\tau)+e_2(t+\tau)+e_3(t+\tau)+e_1(t+2\tau)+e_2(t+2\tau)-e_3(t+2\tau)}{6} \tag{6}$$

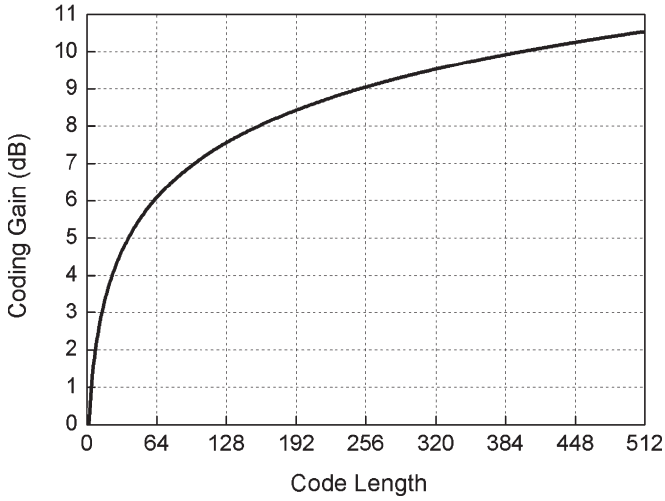

Fig. 2. Amount of SNR enhancement (coding gain) from the scs used in the OTDR measurement, as a function of the code length.

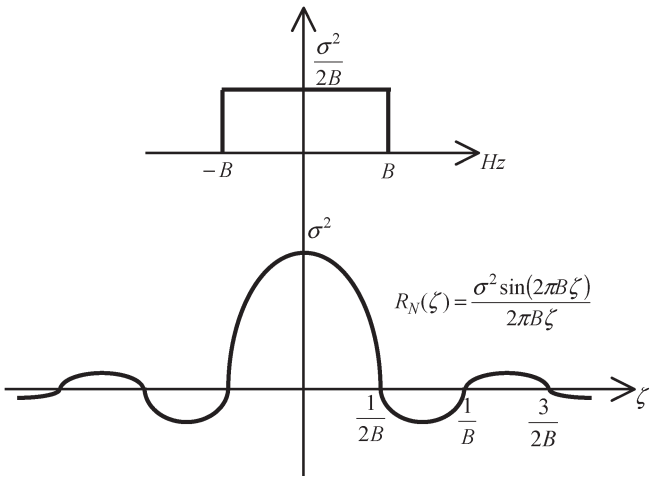

Fig. 3. Frequency response of the ideal band-limited receiver and the autocorrelation function of the noise from the receiver.

that $E\{e_N(t)e_N(t+\varsigma)\} = R_N(\varsigma) = 0, (\varsigma \neq 0)]$ to

$$\frac{4\sigma^2}{(L+1)^2}. \tag{17}$$

From this, finally, we can obtain the following expression for the coding gain of an sc-OTDR with code length $= L$:

$$\frac{\sqrt{\frac{\sigma^2}{L}}}{\sqrt{\frac{4\sigma^2}{(L+1)^2}}} = \frac{L+1}{2\sqrt{L}} \tag{18}$$

Fig. 2 illustrates the amount of SNR enhancement of an sc-OTDR compared to that of a conventional averaging OTDR as a function of the code length in decibel scale $(10 \times \log)$. This coding gain is identical to the result that can be found in the spatial-domain analysis of the Hadamard transform for spectrometry applications [7].

Note that in deriving (17) and (18), we assumed a receiver with an infinite bandwidth. Different from the spectrometry application where the coding is applied in space domain, noise

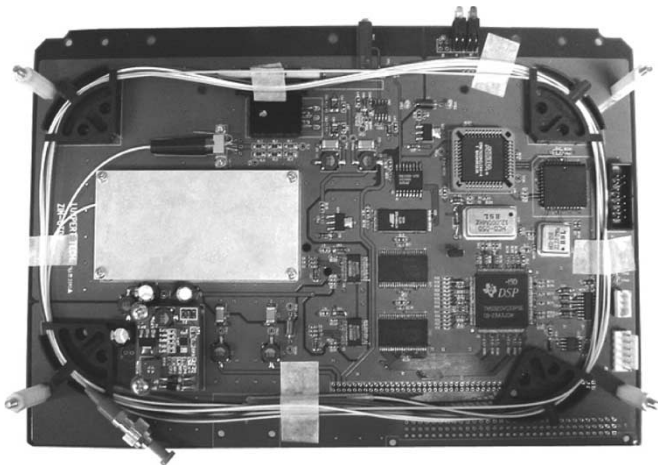

Fig. 4. Picture of the developed OTDR board.

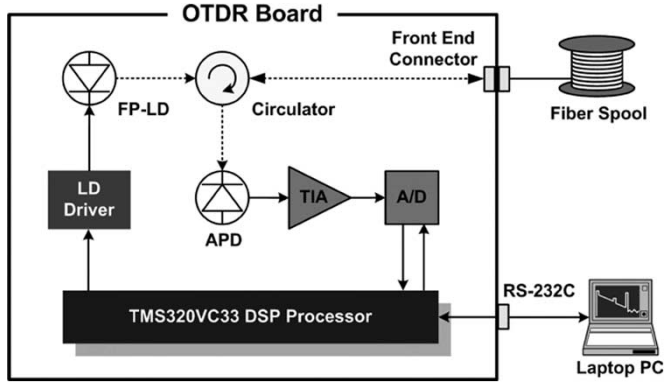

Fig. 5. Schematic diagram of the experiment.

samples adjacent in the time domain are correlated due to the finite bandwidth of the receiver. Considering the nonzero autocorrelation values among the noise samples in the time-domain application of the scs, the complete coding gain of length L can be obtained as

$$\frac{\sqrt{\frac{\sigma^2}{L}}}{\sqrt{\frac{4}{(L+1)^2}\left\{\sigma^2 - \frac{1}{L^2}\sum_{i=1}^{L-1}(L-i)R_N(i\tau)\right\}}} = \frac{\frac{L+1}{2\sqrt{L}}}{\sqrt{1 - \frac{1}{L^2\sigma^2}\sum_{i=1}^{L-1}(L-i)R_N(i\tau)}}. \tag{19}$$

From (19), we can see that the SNR of the finally restored trace depends both on the probe pulsewidth and the autocorrelation function of the receiver noise. Further analysis can be carried out by assuming the frequency response of the receiver to be an ideal low-pass filter (Fig. 3). In this case, the coding gain can be expressed as

$$\frac{\frac{L+1}{2\sqrt{L}}}{\sqrt{1 - \frac{1}{L^2}\sum_{i=1}^{L-1}(L-i)\frac{\sin(2i\pi B\tau)}{2i\pi B\tau}}} \tag{20}$$

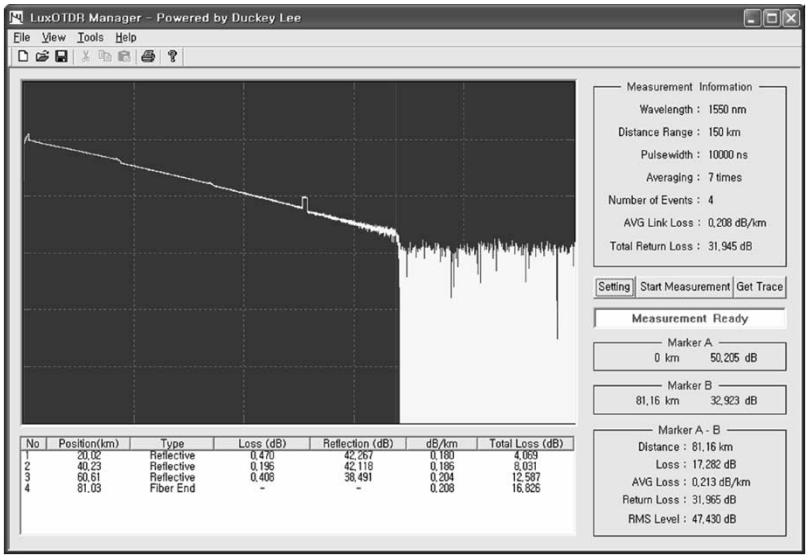

Fig. 6. PC software developed to control the OTDR board, decode the coded traces, and analyze the final trace.

where B is the receiver bandwidth. From Fig. 3 and (20), it is worth noting that it is possible to see that one can get additional improvement in the coding gain from the receiver bandwidth optimization—on top of the pure coding gain attained from (18). For example, with τ, B as the probe pulsewidth, and receiver bandwidth, we get the maximum coding gain from the bandwidth optimization when

$$(n-1)\tau \leq \frac{1}{2B}. \tag{21}$$

Meanwhile, the coding gain is minimized when

$$\tau = \frac{3}{4B}. \tag{22}$$

Note that the additional coding gain from the bandwidth optimization is much smaller when compared to the pure coding gain in Fig. 2 but is not a negligible quantity ($-0.1 \sim 1$ dB).

IV. Experiments

To verify the SNR-enhancement effect in the sc-OTDR, we developed an OTDR board that could modulate probe pulses according to the given code sequences, sample the measured trace, and transmit the sampled data to a PC. The measured traces are transmitted to the PC using RS-232C, and the final trace is restored and displayed at the PC. Fig. 4 shows the developed OTDR board, and Fig. 5 shows a block diagram of the experimental arrangement.

Texas Instrument's Digital Signal Processor (DSP) (TMS320VC33) was used to perform pulse coding, trace acquisition, averaging operation, and data communications. A Fabry–Pérot laser diode (FP-LD) and an avalanche photodiode (APD) were used as the optical source and detector, respectively. The electrical bandwidth of the receiver was ~ 5 MHz, which is proper for probe pulsewidths ≥ 200 ns.

Fig. 6 shows the PC software developed to control and communicate with the sc-OTDR board, to restore the final trace from the coded traces, and to display the event table that is calculated in the software automatically from the final trace.

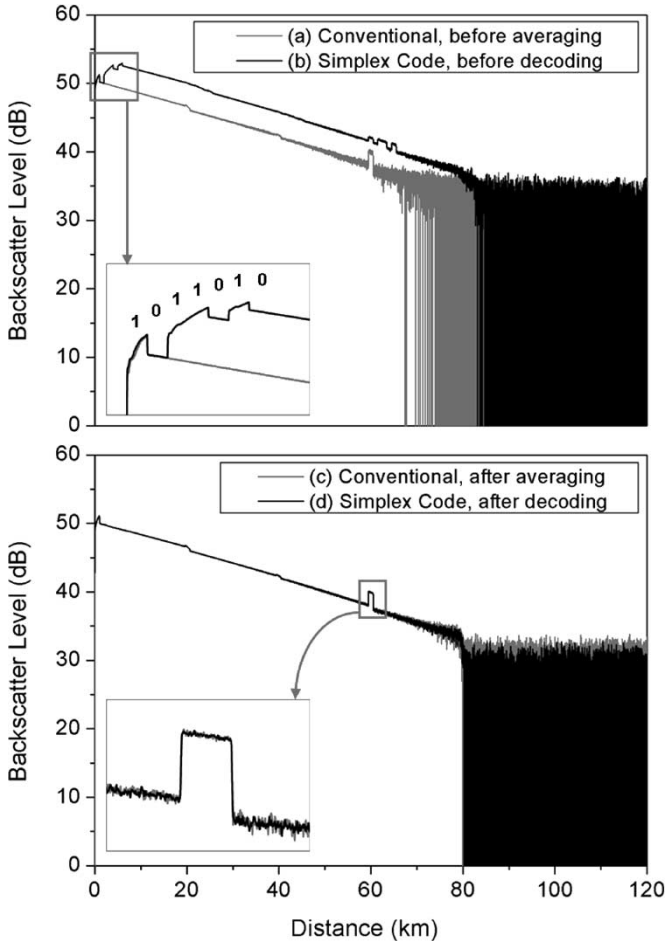

Fig. 7. Experimental results obtained using 7-bit scs and 10-μs bit duration.

For a specific experiment, four spools of 20-km single-mode fiber were connected to the board using fiber connection/physical contact (FC/PC) connectors, while the end of the

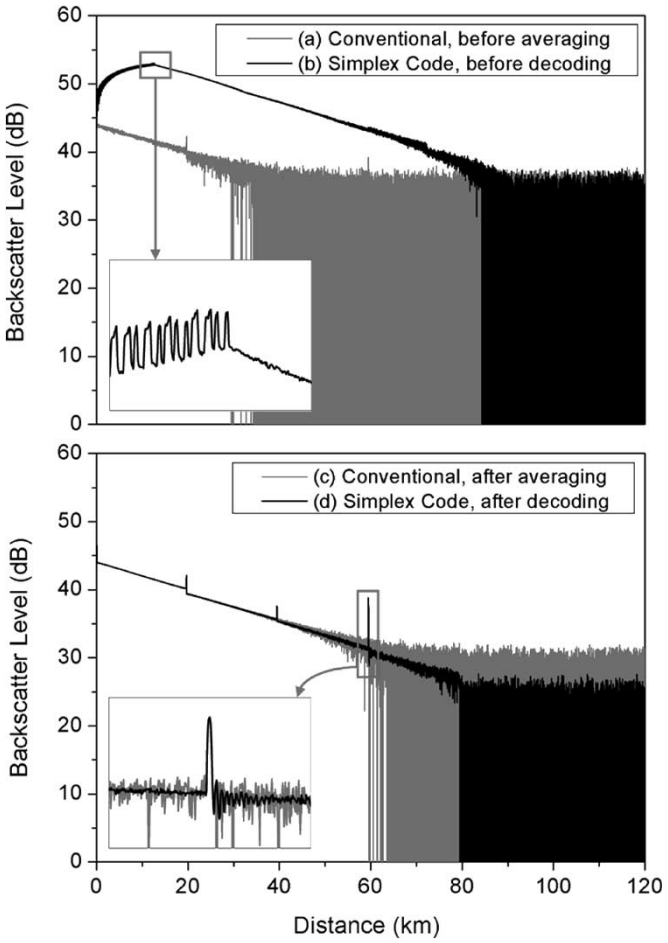

Fig. 8. Experimental results obtained using 255-bit scs and 0.5-μs bit duration.

link was terminated with a fiber connection/angled physical contact (FC/APC) connector.

In Fig. 7, we illustrated experimental results obtained with 7-bit simplex codes at 10-μs unit pulse width. Conventional single-pulse traces (gray line) are displayed together with the simplex-coded traces (black line). Fig. 7(c) shows the final trace averaged from seven single-pulsed traces. To compare, in Fig. 7(d), we plotted the final trace of sc-OTDR decoded from seven simplex-coded traces. With the same measurement time (seven probe shots for both), the final trace obtained using simplex codes showed 2.3 dB lower noise level than the single-pulse averaged trace [the noise levels have been determined by calculating the root-mean-square value of the trace samples after the fiber end (80–120 km)]. It is worth noting that Fig. 7(a) and (b) shows OTDR traces measured before the averaging (a, with a conventional single pulse) or the decoding (b, with a simplex code: code word 1 011 010) process. As can be seen from the figure, the coded trace is composed of a noncoherent superposition of four delayed copies of the single-pulsed trace, where the delay times (locations) of the copies correspond to the 1s in the code word [Fig. 1 and (2)].

For another example, Fig. 8 illustrates experimental results obtained using 255-bit simplex codes at 0.5-μs bit duration. Fig. 8(c) illustrates the final trace averaged from 255 single-pulsed traces, while Fig. 8(d) shows the final trace decoded

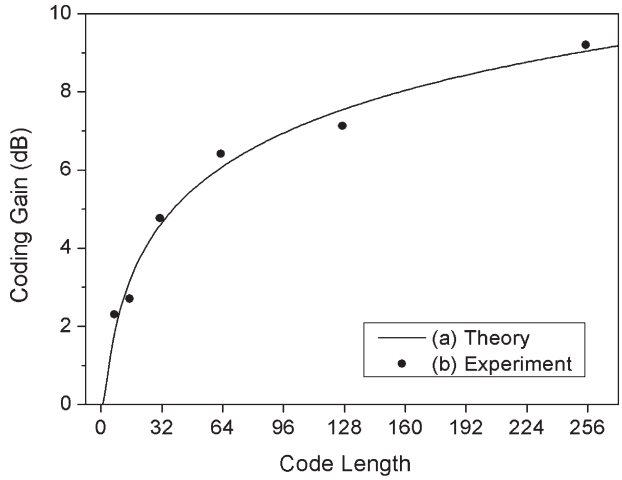

Fig. 9. Coding gains calculated from (a) theory and (b) experimental results.

from 255 simplex-coded traces. Even with the same measurement time (255 probe shots for both) spent, the final trace obtained utilizing the simplex codes exhibited 9.2 dB lower noise level (equivalently, coding gain of 9.2 dB) than the conventional single-pulse averaged trace. Note that the difference of the noise levels is shown as 4.6 dB in the figure since the traces were displayed using the general one-way $(5 \times \log_{10})$ scale for OTDR.

In addition to these two illustrated examples (7- and 255-bit simplex codes), we performed similar experiments with 15-, 31-, 63-, and 127-bit simplex codes. Illustrated in Fig. 9 were the coding gains obtained from experiments at different code lengths. As can be seen, excellent agreement with the theoretical coding gains has been observed over the entire range of code lengths.

V. Conclusion

We proposed a generalized procedure to fully analyze the SNR enhancement and the noise characteristics of a noncoherent simplex-coded OTDR. Experimental procedures and practical considerations have been detailed—including practical issues such as the receiver bandwidth optimization—supporting the constructed theory. Developing an in-house OTDR board with pulse-modulation capability, we experimentally demonstrated an SNR improvement of up to 9.2 dB by applying 255-bit scs, in excellent agreement with the theoretical expectations.

References

[1] K. Okada, K. Hashimoto, T. Shibata, and Y. Nagaki, "Optical cable fault location using correlation technique," *Electron. Lett.*, vol. 16, no. 16, pp. 629–630, Jun. 1980.

[2] A. S. Sudbo, "An optical time-domain reflectometer with low-power InGaAsP diode lasers," *J. Lightw. Technol.*, vol. LT-1, no. 4, pp. 616–618, Dec. 1983.

[3] P. Healey, "Review of long wavelength single-mode optical fiber reflectometry techniques," *J. Lightw. Technol.*, vol. LT-3, no. 4, pp. 876–886, Aug. 1985.

[4] M. Nazarathy, S. A. Newton, R. P. Giffard, D. S. Moberly, F. Sischka, W. R. Trutna, Jr., and S. Foster, "Real-time long range complementary correlation optical time domain reflectometer," *J. Lightw. Technol.*, vol. 7, no. 1, pp. 24–38, Jan. 1989.

[5] M. D. Jones, "Using simplex codes to improve OTDR sensitivity," *IEEE Photon. Technol. Lett.*, vol. 5, no. 7, pp. 822–824, Jul. 1993.
[6] J. A. Decker, Jr., "Experimental realization of the multiplex advantage with a Hadamard- transform spectrometer," *Appl. Opt.*, vol. 10, no. 3, pp. 510–514, Mar. 1971.
[7] M. Harwit and N. J. Sloane, *Hadamard Transform Optics*. New York: Academic, 1979.
[8] E. E. Fenimore and G. S. Weston, "Fast delta Hadamard transform," *Appl. Opt.*, vol. 20, no. 17, pp. 3058–3067, Sep. 1981.

Duckey Lee was born in Seoul, Korea, in 1974. He received the B.S., M.S., and Ph.D. degrees from Seoul National University in 1998, 2000, and 2005, respectively, all in electrical engineering.

In 2005, he joined Korea Telecom, Seoul, where he is currently a Senior Researcher. His research interests include applied photonic systems and security in fixed mobile convergence network.

Hosung Yoon (S'99–M'05) was born in Busan, Korea, on 1975. He received the B.S., M.S., and Ph.D. degrees from Seoul National University, Seoul, Korea, in 1998, 2000, and 2005, respectively, all in electrical engineering.

Since 2005, he has been a Senior Researcher at the Broadband Convergence Network (BcN) Business Unit, Korea Telecom, Daejeon, Korea. His current research interests include advanced optical modulation format, optical access network, fiber amplifiers, and fiber-optic instrumentation.

Pilhan Kim received the B.S., M.S., and Ph.D. degrees in electrical engineering from Seoul National University, Seoul, Korea, in 2000, 2002, and 2005, respectively.

He is currently with Seoul National University, where he is now working as a Postdoctoral Researcher in the optical communication systems laboratory. His research interests include various optical amplifiers such as erbium-doped fiber amplifiers (EDFAs), thulium-doped fiber amplifiers (TDFAs), and Raman from the perspective of bandwidth expansion, efficiency enhancement, transient gain-control methods, optical time-domain reflectometer (OTDR) techniques for distributed-sensing applications, and *in vivo* optical imaging techniques for medical applications. Since 2000, he has published 29 international journal and conference papers in these areas.

Jonghan Park received the B.S. and M.S. degrees in electrical engineering from Seoul National University, Seoul, Korea, in 2002 and 2004, respectively. He is currently working towards the Ph.D. degree in electrical engineering and computer sciences at the same university.

His research interest includes fiber lasers, optical waveguide amplifiers, analysis of various optical noise, fiber sensor, and polarization effects such as polarization-mode dispersion (PMD). Thus far, he has (co)authored 17 international journal and conference publications in this field.

Namkyoo Park (S'90–M'95) received the B.S. and M.S. degrees in physics from Seoul National University, Seoul, Korea, and Brown University, Providence, RI, in 1987 and 1988, respectively. He received the Ph.D. degree in applied physics from California Institute of Technology, Pasadena, in 1994.

After receiving the Ph.D. degree in 1994, he worked in the Specialty Optical Fiber Division of Lucent Bell Laboratories, Murray Hill, NJ, before his short stay at Samsung Electronics (1996–1997). He joined the School of Electrical Engineering and Computer Science (EECS), Seoul National University, in 1997, where he is currently an Associate Professor leading his research group, which was selected by the Korean Ministry of Science and Technology as a National Research Laboratory for next-generation optical amplifiers. With over 15 years of research experience in the area of fiber optics, he has authored/coauthored more than 160 international journal/conference publications, book chapters, and patents. During the past few years, his research efforts have been focused on Raman amplifiers, thulium-doped fiber amplifier (TDFA), optical code division multiple access (OCDMA), polarization mode dispersion (PMD), multilevel transmission, nanocluster Si erbium-doped waveguide amplifier (EDWA), and smart applications of OTDR. He is an Associate Editor of *Optical Fiber Technology* (Elsevier).

Dr. Park is currently an Associate Editor for IEEE PHOTONICS TECHNOLOGY LETTERS.